Trends in the energy dependence of strong interaction characteristics at ultra-high energies

1973 J. Phys. A: Math. Nucl. Gen. 6 1078

(http://iopscience.iop.org/0301-0015/6/7/028)

J. Phys. A: Math., Nucl. Gen., Vol. 6, July 1973. Printed in Great Britain.

Trends in the energy dependence of strong interaction characteristics at ultra-high energies

R H Vatcha and B V Sreekantan
Tata Institute of Fundamental Research, Bombay-5, India

Received 7 December 1972

Abstract. The trends in the energy dependence of strong interaction characteristics that reveal themselves when an attempt is made to bring about a closer agreement between experimentally observed size dependence of several properties of high energy hadrons in air showers and the corresponding Monte Carlo simulations, are discussed. The discussion shows the need for an increase in the inelasticity and interaction cross section of both pions and nucleons at ultra-high energies, as also an increase in the cross section for the production of nucleon–antinucleon pairs and also the need for postulating a process similar to the gammaization process of Nikolsky according to which a considerable fraction of energy is transferred to the soft component by-passing the normal pionization.

1. Introduction

In two earlier papers (Vatcha and Sreekantan 1973a, b, to be referred to as I, II) we have presented experimental results on the high energy hadron component of extensive air showers and from a comparison of the results with expectations based on Monte Carlo simulations have come to the conclusion that several properties of air showers cannot be explained in a consistent manner within the framework of the characteristics of ultra-high energy interactions extrapolated from low energies. We have also shown that a change of primary composition alone in the energy range 10^{14}–10^{16} eV is unable to explain the observations and that certain drastic changes are essential in strong interaction characteristics at ultra-high energies. In particular, we have demonstrated from the behaviour of the charge to neutral ratio of hadrons at high energies, that there has to be a considerable increase in the cross section for the production of $N\bar{N}$'s and also from the behaviour of the fractional hadron energy spectrum either the inelasticity or interaction mean free path or both have to change necessarily at very high energies compared to machine energies.

In this paper we present a discussion of the trends in the characteristics of interactions at ultra-high energies ($\gtrsim$ a few TeV) that reveal themselves when an attempt is made to adjust the parameters of high energy collisions in such a way that there is a better agreement between the expectations on the basis of Monte Carlo simulations and experimental results on high energy hadrons. In adjusting these parameters, we have been governed by the other properties of air showers also, like the size variation of the low energy hadrons and muons, and of the ultra-high energy muons and the relation between the primary energy and the shower size. Obviously such an adjustment is a synthetic one and cannot be claimed to be unique. It may turn out that all the changes

visualized are not strictly necessary or even that all of them may not be entirely sufficient and also all the properties of air showers may not be fully explained. In fact we find that while it has been possible to achieve, on the basis of these adjustments of parameters, a much closer agreement in certain properties and the right trends, regarding certain other properties discrepancies still remain, though they do not widen. The exercise has in the main shown that the directions in which changes are introduced are the right ones and calculations with further adjustment of parameters should result in a much better over-all agreement. To pursue further the adjustment of parameters, the limitation is really the computer time required, which is enormous. Also experimental results of much higher precision are necessary before further refinements of calculations are attempted.

2. Guidelines for adjustment of collision parameters

The experimentally observed features of high energy hadrons which have shown considerable departure from the predictions of simulations based on 'normal models' of high energy interactions are: (i) the hadron energy spectrum is very steep and there is evidence for a further steepening of the spectrum with increasing size; (ii) the absolute numbers of hadrons observed experimentally are less by almost an order of magnitude; (iii) the charged to neutral ratio of hadrons in EAS has a rather low value (~ 6) and decreases further (~ 3) at higher sizes; (iv) the fractional hadron energy spectrum falls below the calculated spectrum of survivors and is different for different sizes.

While these features suggested the broad directions in which changes had to be introduced in collision parameters, it was necessary to go through a number of trial and iterative stages of calculations before a set of parameters could be arrived at, which, when adopted, gave a closer agreement between the Monte Carlo simulations and the experimental results. The steepening of the hadron spectrum at high energies suggested an increase of inelasticity and a reduction of the interaction mean free path. For energies up to 100 GeV, the study of the detailed cascade profiles of both charged and neutral induced hadron cascades in the multiplate cloud chamber had shown identical features and required an inelasticity less than 0·5 (Vatcha *et al* 1972). Since at these energies, the charged hadrons are mostly pions, this result also meant that at energies up to 100 GeV, the interactions of pions also should be treated as partially inelastic. A value of $\eta_N = \eta_\pi = 0{\cdot}35$ was therefore adopted. Since the steepening of the hadron spectrum was apparent from 100 GeV onwards and since the C/N ratio showed a rapid depletion of pions at energies greater than 200 GeV, both λ_π and η_π were radically changed over the narrow interval 10^{11} to 2×10^{11} eV. η_π was linearly increased from 0·35 to 0·9 and λ_π was decreased from 130 g cm^{-2} in air to 70 g cm^{-2}. In the case of nucleons it was not necessary to change the parameters over a narrow interval. The inelasticity of nucleons η_N was increased from 0·35 to 0·5 over the energy range 10^{11} to 10^{12} eV which is not in conflict with most of the experiments on hadrons in this energy range. η_N was further increased from 0·5 to 0·9 over the energy interval 10^{12} to 5×10^{14} eV and was held at this high value for higher energies. This increase was dictated by the consideration that the fractional hadron energy spectrum is different for showers of size less than and greater than 3×10^5. The interaction mean free path for nucleons λ_N was changed from 80 g cm^{-2} at $E < 10^{11}$ eV to 65 g cm^{-2} at $E \geqslant 10^{12}$ eV from similar considerations. It may be mentioned that there is some indication from the distribution of the points of interactions in the cloud chamber plates of cascades of energy greater than

10^{12} eV, for an interaction mean free path smaller than at lower energies. The proton satellite experiments of Akimov *et al* (1969) also show an increase in the cross section for proton–carbon interactions at energies greater than 6×10^{11} eV. From a comparison of the unaccompanied hadron energy spectra at various depths in the atmosphere Yodh *et al* (1972) have shown that the $\sigma_{\text{p-air}}$ (inelastic) increases from 250 mb at 10^{11} eV to 350 mb at $E \gtrsim 3 \times 10^{13}$ eV. These drastic changes in inelasticity and interaction mean free path resulted in the depletion of high energy muons and contradicted experimental observations unless a rapid increase of multiplicity was employed at very high energies. For this reason the multiplicity was taken at all energies to be proportional to $E^{1/2}$, since at lower energies it makes very little difference whether the multiplicity is ln E, $E^{1/4}$ or $E^{1/2}$, as far as the present calculations are concerned. A large multiplicity is indicated at ultra-high energies also because a rapid fragmentation of energy is expected at such energies. However, because of the rapid fractionation of energy, and to explain the rather slow rate of increase of high energy muons with shower size observed in the KGF experiments, it was necessary to reduce the probability of formation of isobars at $E > 10^{12}$ eV. When trials were made incorporating these changes it turned out that the relation between the primary energy and the shower size at the observational level was seriously affected. For a given primary energy the shower size was much too small compared to what was found by a direct comparison of the primary spectrum derived by the satellite experiment and the size spectrum determined at Ooty. In order to restore this relation it became essential to introduce a process similar to that of the gammaization process of Nikolsky (1967) according to which a considerable fraction of energy is transferred directly into the soft component by-passing pionization. The possibility of gammaization is also indicated from the feature of a rapid absorption of cascades of energies greater than 1 TeV which has been observed by Vatcha *et al* (1972).

The rather low value of the charge to neutral ratio observed by us for hadrons of energy greater than 25 GeV in showers of size greater than 3×10^5 when the number of hadrons is of the order of several hundred clearly demonstrates, as pointed out in the earlier paper, the presence of a large number of $N\bar{N}$'s among the hadrons. The time structure experiments of hadrons in air showers carried out at Ooty (Tonwar and Sreekantan 1971) have shown that there is a considerable increase in the cross section for the production of $N\bar{N}$'s at energies of the order of a few hundred GeV. There is confirmation for this trend from the recent ISR experiments. If such an increase in the cross section for the production of $N\bar{N}$'s is taken into account, then as shown by Murthy (1967) the rather low value of the C/N ratio can be explained even in conventional models of high energy interactions. However, our observation that this ratio decreases further to a value of $3{\cdot}2 \pm 0{\cdot}5$ in showers of size greater than 3×10^5 has very important implications and cannot be explained in the framework of the conventional models even taking into account increase of $N\bar{N}$ production. It is obvious that such a size dependent effect has to be traced to collisions which occur in showers of size greater than 3×10^5 and are not present in showers of smaller size, which means collisions of energy greater than about 5×10^{14} eV. Such high energy collisions take place only in the early stages of the hadron cascade and therefore high up in the atmosphere. In order to influence the C/N ratio of hadrons of energy as low as 25 GeV at 800 g cm^{-2} considering the very steep hadron energy spectrum, it is necessary that in these collisions a large fractionation of energy takes place and a large number of $N\bar{N}$'s of sufficient low energy are produced to take care of the attenuation in the intervening atmosphere. Under these circumstances the contribution to the hadrons from $N\bar{N}$'s produced in collisions of energy a few TeV and less turns out to be small even if we consider the increase in cross section. We have

therefore used the relations of the type

$$F_r = \frac{1}{1 + (4 \times 10^{14}/E)^3},$$

where E is the incident energy in eV,

$$F_i = \frac{7F_r}{1 + 6F_r},$$

where F_r is the fraction of $N\bar{N}$'s produced and F_i is the fraction of energy going into $N\bar{N}$'s in collisions of energy E.

Thus the parameters of high energy collisions for the final Monte Carlo simulations of the hadron cascades used are:

(i) *Inelasticity*

(*a*) Nucleons: $\eta_N = 0{\cdot}35$ for $E \leqslant 10^{11}$ eV
$= 0{\cdot}35$ to $0{\cdot}05$—linear rise for $E = 10^{11}$ to 10^{12} eV
$= 0{\cdot}5$ to $0{\cdot}9$—linear rise for $E = 10^{12}$ to 5×10^{14} eV
$= 0{\cdot}9$ for $E > 5 \times 10^{14}$ eV.

(*b*) Pions: $\eta_\pi = 0{\cdot}35$ for $E \leqslant 10^{11}$ eV
$= 0{\cdot}35$ to $0{\cdot}9$ linear rise for $E = 10^{11}$ to 2×10^{11} eV
$= 0{\cdot}9$ for $E > 2 \times 10^{11}$ eV.

(*c*) Fluctuations: If the average value is $\bar{\eta}$, the probability distribution is given by a sine function normalized between extreme values of $\frac{1}{2}(3\bar{\eta}-1)$ to $\frac{1}{2}(\bar{\eta}+1)$ corresponding to argument values of 0 and π of the sine function.

(ii) *Interaction mean free path*

Nucleons: $\lambda_N = 80$ g cm^{-2} for $E \leqslant 10^{11}$ eV
$= 80$ g cm^{-2} to 65 g cm^{-2}—linear decrease from $E = 10^{11}$ to 10^{12} eV
$= 65$ g cm^{-2} for $E > 10^{12}$ eV.

Pions: $\lambda_\pi = 130$ g cm^{-2} air for $E \leqslant 10^{11}$ eV
$= 130$ g cm^{-2} to 70 g cm^{-2}—linear decrease from 10^{11} to 2×10^{11} eV
$= 70$ g cm^{-2} for $E > 2 \times 10^{11}$ eV—fluctuations by Monte Carlo methods.

(iii) *Multiplicity*

In collisions of nucleons: $M_N = 2{\cdot}0 + 0{\cdot}2E^{1/2}$.
In collisions of pions: $M_\pi = 2{\cdot}0 + 0{\cdot}3E^{1/2}$.
Fluctuations are box type from $M/2$ to $3M/2$.

(iv) *Gammaization*

30% of available energy is distributed into 6 γ rays of equal energy on the average. The probability of gammaization increases from zero for $E \leqslant 10^{12}$ eV to 1 for $E \geqslant 10^{13}$ eV.

(v) *Isobar formation*

The probability of formation is 50% for $E \leqslant 10^{12}$ eV and decreases linearly to 0 at $E \geqslant 5 \times 10^{14}$ eV. When an isobar is formed, 20% of the total energy is available to a single fireball, and the remaining 80% is divided between a surviving nucleon (whose energy is determined by η_N) and three decay pions of equal energies on the average. The nucleon retains at least 16% of the total energy on the average even at the highest energies.

(vi) *Energy and p_T distribution of secondaries*
At $E > 8 \times 10^{14}$ eV there is equipartition of energy. At lower energies the same as Murthy *et al* (1968a, b).

(vii) *Nucleon–antinucleon production*
The fraction of $N\bar{N}$'s is given by

$$F_r = \frac{1}{1 + (4 \times 10^{14}/E)^3}$$

where E is the incident hadron energy in eV. The fraction of energy given to $N\bar{N}$ pairs is

$$F_i = \frac{7F_r}{1 + 6F_r}.$$

3. Results of Monte Carlo simulation and comparison with observation

In order to compare the results of simulations of EAS with experimental results, the simulated showers were generated from a primary energy spectrum from 10^{14} to 10^{16} eV and the resulting showers classified according to their size at 800 g cm^{-2} as in the experimental data. Full details are available in Vatcha (1972). The effects of a mixed composition have not been considered as the objective of the calculations is only to understand trends.

3.1. Relation between primary energy and shower size

The present calculations led to a conversion factor of 4·3 GeV per particle between the primary energy and the shower size at 800 g cm^{-2}. A value of about 2 Ge V per particle is obtained from a comparison between the primary energy spectrum directly measured in the proton satellite by Grigorov *et al* (1971) and the size spectrum measured by us at Ooty. Considering the uncertainties in flux due to solid angle factors which depend upon angular distribution of showers as well as the statistical errors in the determination of size etc, and also the uncertainties in the derivation of the primary spectrum in the satellite experiment, the discrepancy may not be very significant. The agreement can be improved by a readjustment of parameters especially the extent of gammaization, and energy fractionation.

3.2. Integral energy spectrum of hadrons in EAS

The integral energy spectrum of hadrons obtained on the basis of simulated showers is plotted in figure 1 corresponding to average weighted primary energy values of $1{\cdot}6 \times 10^5$ GeV, 5×10^5 GeV, $1{\cdot}6 \times 10^6$ GeV and 5×10^6 GeV. In the same figure the simulations of Murthy *et al* (1968a, b) and of Greider (1971) are also shown. The notations have been described in paper II. The experimental spectra obtained for the two size groups of $3{\cdot}2 \times 10^5$ or above and less than $3{\cdot}2 \times 10^5$ corresponding to average primary energies of 4×10^5 GeV and 3×10^6 GeV (using a conversion factor of 4·3 GeV/particle) are also shown. Even the lowest values given by Murthy *et al* for hadron numbers are larger than observed by at least an order of magnitude. The calculations of Greider give a slightly better agreement in number at energies of about 100 GeV or less, but because of the

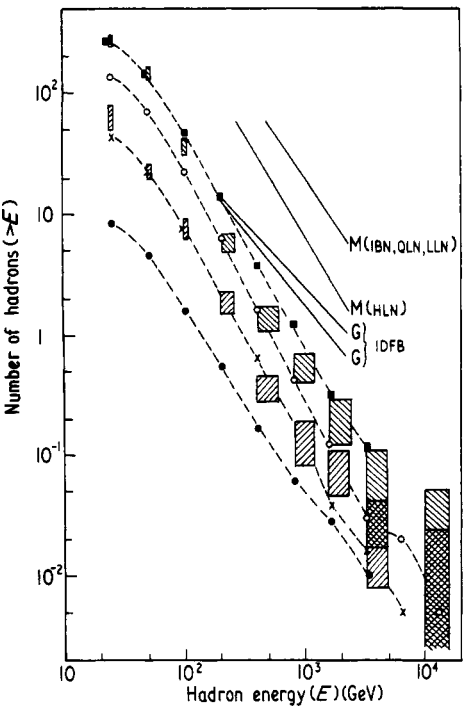

Figure 1. The integral energy spectrum of hadrons in EAS initiated by primaries of different energies. Average weighted primary energy values of $1{\cdot}6 \times 10^5$ GeV (●), $5{\cdot}0 \times 10^5$ GeV (×), $1{\cdot}6 \times 10^6$ GeV (○), $5{\cdot}0 \times 10^6$ GeV (■) are plotted. The results from the present Monte Carlo simulations indicate a steepening of the spectra with increasing primary energy. The results from the simulations of Murthy *et al* (curve M) and Greider (curve G) are also shown for primaries of energies of 10^6 GeV. The experimental values obtained from an earlier paper are also indicated: average weighted primary energy values of 3×10^6 GeV (▧) and 4×10^5 GeV (▨) are shown.

flatter spectrum the discrepancy increases at larger energies. There is fair agreement between experimental results and the predictions from the present calculations which also show the tendency for the energy spectrum to steepen with increasing primary energy.

In figure 2 the exponent γ of the integral energy spectrum of hadrons for different shower size groups is plotted and it is seen that the trend of steepening of the hadron spectrum with increasing size is reproduced to some extent although it is slower than experimental results indicate. This feature is a reflection of the hypothesis of strong energy fractionation at ultra-high energies with increasing dissipation of energy in the soft component, and can be adjusted further.

3.3. Size variation of the number of hadrons

In figure 3(*a*) the calculated number of hadrons for specific sizes is compared with experimental results shown by curves for different hadron energies. There is reasonable agreement at lower hadron energies but the calculated rate of increase of number is steeper than experimental ones especially at higher energies. The calculated rates are

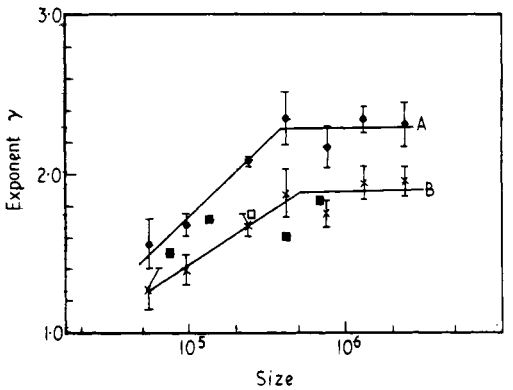

Figure 2. The variation of the exponent γ of the integral energy spectrum of hadrons with shower size in the range $E = 50-800$ GeV. The experimental curve A is obtained without considering the effects of systematic errors whereas the experimental curve B is obtained assuming maximum possible systematic errors. The points refer to the results of the present simulations.

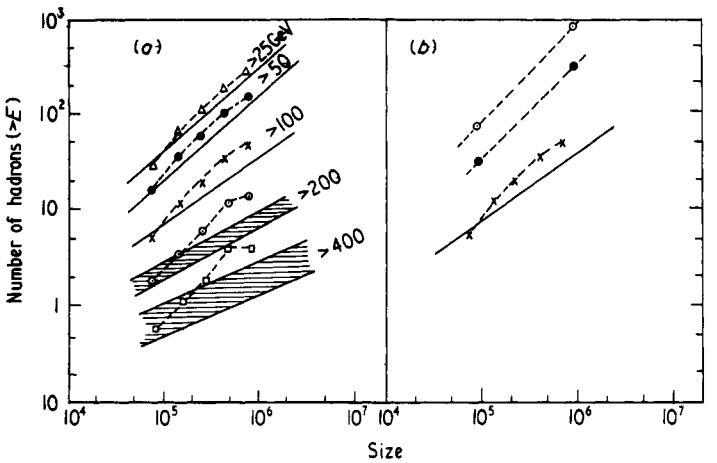

Figure 3. The variation of the number of hadrons of different threshold energies with shower size. The results of the present simulations are shown by points and the curves are obtained from experimental values given in an earlier paper. Figure 3(*a*) presents the results for hadrons with threshold energies from 25 GeV to 400 GeV. In figure 3(*b*) a comparison is made between the experimental results for hadrons of energies greater than 100 GeV (full line) with the present simulations (×) as well as earlier simulations of Murty *et al* (○, without $N\bar{N}$, ⊙ with $N\bar{N}$).

slower for hadron energy thresholds of 800 GeV and 1600 GeV. It is significant that the present calculations give absolute numbers much closer to experimental numbers (within a factor of 2 at all hadron energies) than the previous calculations shown for hadrons of energy greater than 100 GeV in figure 3(*b*). The present calculations however do not indicate any break in the slope at a size of about 3×10^5 even for the highest hadron energies for which there is some experimental evidence.

3.4. The charge to neutral ratio of hadrons

In figure 4 the charge to neutral ratio obtained from the simulations as a function of energy for various size groups is plotted. The experimental points for two size groups (ie $\geqslant 3{\cdot}2 \times 10^5$ and $< 3{\cdot}2 \times 10^5$) are also shown. While the trend for the ratio to decrease

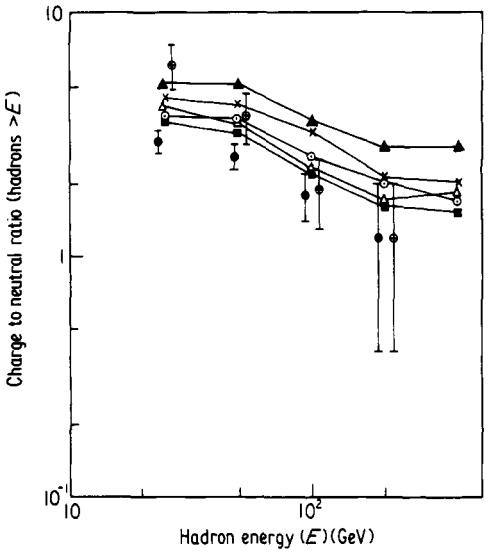

Figure 4. The variation of the charged to neutral ratio of hadrons with hadron energy for showers of different sizes. The five curves are obtained from the present simulations corresponding to different size groups: ▲ $5{\cdot}6 \times 10^4$–10^5; × 10^5–$1{\cdot}8 \times 10^5$; ⊙ $1{\cdot}8 \times 10^5$–$3{\cdot}2 \times 10^5$; △ $3{\cdot}2 \times 10^5$–$5{\cdot}7 \times 10^5$; ■ $5{\cdot}7 \times 10^5$–10^6. The experimental values for two size groups are also shown: ⧳ $>3{\cdot}2 \times 10^5$; ⧲ $<3{\cdot}2 \times 10^5$.

with increasing size is reproduced in the present calculations the values are slightly higher for energies greater than 100 GeV compared to the experimental values. The introduction of a small amount of $N\bar{N}$ production at energies of 1 TeV or less as discussed earlier would possibly reduce this discrepancy.

3.5. Variation of the number of muons with size

The calculated number of muons of different energy thresholds (ie 20 GeV, 220 GeV and 640 GeV) for different shower sizes are shown in figure 5. The experimental results of Sivaprasad (1971) with the KGF array for muons of energy greater than 220 and 640 GeV and those of Vernov *et al* (1968) for muons of energy greater than 20 GeV (extrapolated from > 10 GeV muons) are also shown. For low energy muons the agreement is reasonable whereas for high energy muons the calculated size variation is slightly steeper. However, for muons of energies of about 220 GeV or more, the discrepancy in the numbers at any size is less than 50%. The maximum discrepancy is in the number of muons of energy greater than 640 GeV at a size of the order of 10^5, which is a factor of three. These discrepancies could perhaps be reduced by further adjustments of parameters.

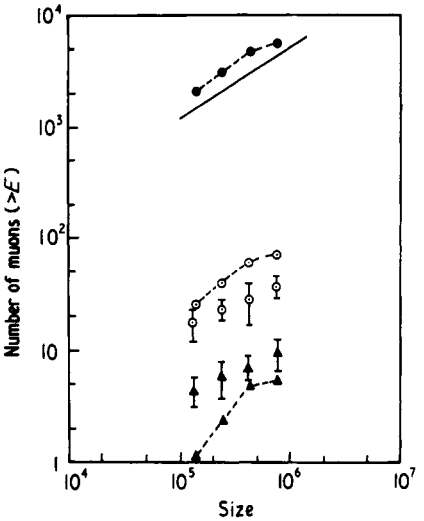

Figure 5. The variation of the number of muons of different threshold energies with shower size. The results of the present simulations are shown by points without error bars. The experimental points with error bars are for high energy muons obtained from the experiment at the Kolar gold fields: ⊖ > 220 GeV; ▲ > 640 GeV. The full line is the experimental curve slightly extrapolated from the data of Vernov *et al.*

3.6. The transverse momentum distribution of very high energy hadrons

In normal models of EAS development the transverse distribution of hadrons from the axis may be regarded as essentially determined by the height of the previous interaction with respect to the observational level and the transverse momentum acquired by the hadron in this interaction. This is because, in the normal models the number of hadrons that leak through from large heights without undergoing interactions is negligible, compared to those coming from interactions further down. In this case the transverse distribution of hadrons can be calculated without going through detailed Monte Carlo simulations. It is convenient to calculate the distribution of the parameter $Y = rE_0$ where r is the distance from the axis and E_0 is the energy of the hadron. The distribution of Y is the result of the distribution of the height of previous interaction and the distribution of the transverse momentum. Thus the differential distribution of 'Y' is given by

$$F(Y)\,\mathrm{d}Y = \int\int f(R)\,\mathrm{d}R\Phi(p_T)\,\mathrm{d}p_T$$

subject to the condition $Y = rE_0 = p_T R$, where r is the distance of the hadron from the core, E_0 is the hadron energy, R is the distance from the last interaction to the observation level and p_T is the transverse momentum given to the hadron. The distribution of R is given by

$$f(R)\,\mathrm{d}R = \mathrm{e}^{-X/\lambda}\frac{\mathrm{d}X}{\lambda}$$

where λ is the hadron interaction mean free path and X is the amount of matter equivalent to the distance R. The distribution of p_T is assumed to be

$$\Phi(p_T)\,\mathrm{d}p_T = \frac{p_T}{p_0}\exp\left(-\frac{p_T}{p_0}\right)\frac{\mathrm{d}p_T}{p_0}.$$

Then

$$F(Y)\,dY = dY\int_0^\infty f\left(\frac{Y}{p_T}\right)\exp\left(-\frac{p_T}{p_0}\right)\frac{dp_T}{p_0^2}.$$

Using the relation† $X = G - X_0\exp[-\{(R+H)/Z_0\}]$ between X (g cm^{-2}) and R (km), where X_0, Z_0 and G are constants, the differential distribution of Y reduces to the form

$$F(Y)\,dY = dY\frac{X_0}{\lambda Z_0 p_0^2}\int_0^\infty \exp\left(-\left[\frac{G}{\lambda}+\frac{Y+p_T H}{Z_0 p_T}+\frac{p_T}{p_0}-\frac{X_0}{\lambda}\exp\left\{-\left(\frac{Y+p_T H}{p_T Z_0}\right)\right\}\right]\right)dp_T$$

where $X_0 = 1075\,\text{g cm}^{-2}$, $Z_0 = 7{\cdot}5\,\text{km}$, $G = 800\,\text{g cm}^{-2}$, $\lambda = 80\,\text{g cm}^{-2}$ and $H = 2{\cdot}2\,\text{km}$.

In figure 6 the expected distribution of Y is plotted for $p_0 = 0{\cdot}25$, 1·0, 5·0 as curves A, B, and C from the above calculations.

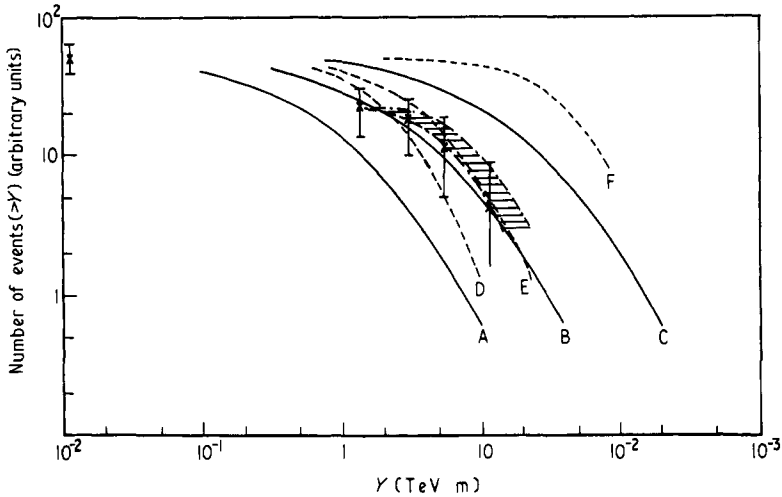

Figure 6. The lateral distribution of cascades of energy greater than 1 TeV associated with EAS. The variable Y is the product of the cascade energy (TeV) and its distance from the shower core (m). The curves A, B and C are obtained for different average p_T values (0·5, 2·0, 10·0 GeV/c respectively) based upon calculations assuming a normal development of EAS. The curves D, E and F are similar curves for average p_T values (0·5, 2·5, 10·0 GeV/c respectively) obtained from the present simulations. The experimental points which are also shown as well as all the curves are normalized at $Y = 0$.

In our case, when we have radically changed the parameters of collisions and introduced large fractionation of energy in the first few collisions at the top of the atmosphere, most of the high energy hadrons at the observational level are due to 'leak throughs' from various levels and especially from the first few interactions in the atmosphere. Because of this reason, it is necessary to obtain the distribution of the transverse displacement or alternatively of the parameter Y only through detailed Monte Carlo simulations. The curves D, E and F in figure 6 are those obtained from such Monte Carlo calculations for primaries in the energy range 10^6–$3{\cdot}2\times10^6$ GeV, weighted according to the primary spectrum. All the curves are normalized at $Y = 0$.

It is seen from figure 6 in which the experimentally obtained distribution of Y is also given for TeV cascades (table 1 of paper I), that in the normal models, the closer

† This approximate relation is obtained from the curve given by Rossi (1965) near the depth of 800 g cm^{-2}.

fit to the experimental points is given by curve B which corresponds to a $\langle p_T \rangle$ value of 2·0 GeV/c, rather than curve A which corresponds to the usually accepted value of 0·5 GeV. However, according to our calculations in which the interaction characteristics are radically different, within errors even the value of 0·5 GeV/c could be accommodated.

In paper II we have seen that the absolute number of high energy hadrons obtained in our experiment is lower than the numbers obtained in other experiments. We would like to remark at this stage that if this difference is attributed to any systematic underestimate of energies, say, by a factor of five, then the experimental distribution of figure 6 would move to the right by this factor and would indicate a mean average transverse momentum of 10 GeV/c even in a normal model of strong interactions. Thus any systematic bias in the hadron energy estimate, if it exists at all, cannot be used to explain away all the changes in the interaction characteristics which have been introduced at ultra-high energies; either $\langle p_T \rangle$ increases very drastically or the inelasticity increases and/or the interaction mean free path decreases.

A reasonably good fit is obtained even with a value of 0·5 GeV/c for $\langle p_T \rangle$ because of the fact that according to our calculations, for the reasons already discussed, high energy hadrons essentially come as 'leak throughs' from higher levels of the atmosphere and are thus effectively spread out. Such a picture also explains the observation that the C/N ratio for hadrons of energy greater than 100 GeV decreases from a value of $2{\cdot}3 \pm 0{\cdot}5$ at $r < 8$ m to $1{\cdot}3 \pm 0{\cdot}5$ at $r > 8$ m since the effective production height of high energy nucleons is higher than that of pions, due to enhanced production of $N\bar{N}$'s in ultra-high energy collisions.

4. Conclusions

It is clear from § 3 that the adjustment of various parameters of high energy collisions has led to a closer agreement between the experimental results on high energy hadrons and muons and the Monte Carlo simulations. It is significant that this adjustment which is mainly guided by the behaviour of the high energy hadrons and muons has not led to any serious contradictions with respect to other properties of air showers. While it is clear that with further adjustment of parameters and more intensive calculations it may become feasible to bring much closer agreement, it is not warranted at the present stage considering the available accuracy of the experimental results. What can be claimed at this stage is that the various changes introduced may be inaccurate in detail, but the general trend is in the right direction. The over-all picture regarding the behaviour of ultra-high energy interactions and the development of hadronic cascades in the atmosphere that emerge from the present study may be stated as follows.

At energies less than 100 GeV, the hadron interactions are only partially inelastic. A large fraction of the energy is still maintained in a 'surviving' hadron which emerges often in an excited isobaric state. As the energy approaches the TeV region, the inelasticity increases slightly and the cross section also increases as more channels become available for interaction. Nucleon–antinucleon pair production starts becoming important at these energies. At the same time, a considerable fraction of the available energy is occasionally given to the soft component by-passing pionization; the probability of this 'gammaization' component (a terminology introduced by Nikolsky) increases with energy. As the energy increases still further the probability of isobar formation reduces so that large fractions of energy are not available to a few secondaries. At the highest energies of about 5×10^5 GeV or more, strong energy fractionation takes

place and isobar formation is not significant. As the inelasticity increases, the fraction of energy available to 'gammaization' also increases. A drastic increase in the production of nucleon–antinucleon pairs occurs around the same energy, and long before this energy is reached, the multiplicity increases proportional to $E^{1/2}$. However, any apparent increase in $\langle p_T \rangle$ at such energies inferred from EAS data is explicable on the basis of an increase in the level of production of high energy hadrons rather than an actual increase in the value of $\langle p_T \rangle$.

References

Akimov V V *et al* 1969 *Proc. 11th Int. Conf. on Cosmic Rays, Budapest* 1969 vol 3 (Budapest: Central Research Institute for Physics) pp 211–4

Greider P K F 1971, *Proc. 12th Int. Conf. on Cosmic Rays, Hobart* 1971 vol 3 (Hobart: University of Tasmania) pp 970–5, 976–81

Grigorov N L *et al* 1971 *Proc. 12th Int. Conf. on Cosmic Rays, Hobart* 1971 vol 5 (Hobart: University of Tasmania) pp 1746–51

Murthy G T 1967 *PhD Thesis* University of Bombay

Murthy G T *et al.* 1968a *Can. J. Phys.* **46** S147–52

—— 1968b *Can. J. Phys.* **46** S159–63

Nikolsky S I 1967 *Sov. Phys.–JETP* **24** 535–45

Rossi B 1965 *High Energy Particles* (New York: Prentice-Hall) p 545

Sivaprasad K 1971 *PhD Thesis* University of Bombay

Tonwar S C and Sreekantan B V 1971 *J. Phys.* A: *Gen. Phys.* **4** 868–82

Vatcha R H 1972 *PhD Thesis* University of Bombay

Vatcha R H and Sreekantan B V 1973a *J. Phys.* A: *Math., Nucl. Gen.* **6** 1050–66

—— 1973b *J. Phys.* A: *Math., Nucl. Gen.* **6** 1067–77

Vatcha R H, Sreekantan B V and Tonwar S C 1972 *J. Phys.* A: *Gen. Phys.* **5** 859–76

Vernov S N *et al* 1968 *Can. J Phys.* **46** S197–200

Yodh G B, Pal Y and Trefil J S 1972 *Phys. Rev. Lett.* **28** 1005–8